Proceedings of the 11th Brazilian Congress of Thermal Sciences and Engineering -- ENCIT 2006
Braz. Soc. of Mechanical Sciences and Engineering -- ABCM, Curitiba, Brazil,- Dec. 5-8, 2006

Paper CIT06-0419

OIL RECOVERY BY A VISCOPLASTIC MATERIAL

Maximilian S. Mesquita[1]
Edson J. Soares[1]
Roney L. Thompson[2]
Márcio S. Carvalho[3]
mesquita@ct.ufes.br
edson@ct.ufes.br
roney@vm.uff.br
msc@mec.puc-rio.br
[1] Department of Mechanical Engineering, Universidade Federal do Espírito Santo, Avenida Fernando Ferrari. s/n, Goiabeiras, 29060-900, Vitória, ES, Brazil.
[2] Laboratório de Mecânica Aplicada, PGMEC, Department of Mechanical Engineering, Universidade Federal Fluminense, Rua Passo da Pátria 156, 24210-240, Niterói, RJ, Brasil.
[3]Department of Mechanical Engineering, Pontifícia Universidade Católica do Rio de Janeiro, Rua Marques de São Vicente 225, 22453-900, Rio de Janeiro, RJ, Brazil.

Abstract. Oil recovery in porous media is an important problem in oil industry nowadays. In the micro-scale of this media, interfacial forces have a strong influence on the recovery efficiency. An interesting path to investigate is how rheological properties of non-Newtonian fluids can influence on this efficiency. An elliptic mesh generation technique, with the Galerkin Finite Element Method is used to compute the interface of the flow problem of a viscoplastic material displacing oil in a capillary tube. The constitutive equation is a Generalized Newtonian Fluid (GNF) with the viscosity function proposed by Papanastasiou (1987). The results were given as a function of a non-Newtonian Capillary number and the dimensionless yield stress. The goal of the present work is to study flow patterns, configuration of the interface between the two phases, and fraction of the mass of oil deposited at the wall, as functions of the dimensionless numbers cited. As the displacing fluid departs from Newtonian behavior the fraction of the mass deposited on the tube wall decreases and the shape of the interface becomes flatter.

Keywords: *liquid-liquid displacement, non-Newtonian liquids, Papanastasiou viscosity function , finite element method, free surface flows*

1. Introduction

The present paper deals with the displacement of a liquid, initially occupying the interior of a tube, by another liquid which is immiscible with the first. Practical applications include the flow through porous media during enhanced oil recovery and the cementation process of production and injection wells. Comprehensive reviews on this subject are available in the literature. In these processes, it is important to understand the mechanism of liquid displacement and to determine the amount of liquid that is left behind adjacent to the wall. The configuration of the interface between the two liquids depends on the force balance near the interface, which is the focus of the present study. Most of the related work found in the literature deals with the case of a gas displacing a viscous liquid, going back to the pioneer work of Fairbrother and Stubbs (1935) and Taylor (1961). In the experiments reported in these early papers, the Reynolds number was kept small enough to assure negligible inertial effects. The main goal was to determine the fraction of mass deposited on the tube wall *m*, which, with the aid of the mass conservation principle, can be written as a function of the velocity of the tip of the interface U and the mean velocity $\bar{u}$ of the liquid ahead of the gas-liquid interface, viz.,

$$m = \frac{U - \bar{u}}{U} \tag{1}$$

Taylor (1961) studied the dependence of the mass fraction on the *capillary number* $Ca \equiv \mu U/\sigma$, where μ and σ are the liquid viscosity and surface tension, respectively. His analysis indicated that the amount of liquid deposited on the wall rises with the interface speed, and that *m* tends asymptotically to a value of 0.56 as *Ca* approaches 2. Working on the same problem, Cox (1962) studied the mass fraction over a wider range of the capillary number, and also observed that *m* reaches an asymptotic value at a high capillary number. However, he showed that this asymptotic value was 0.60 as *Ca* approached 10. Using the lubrication approximation, Bretherton (1961) derived a theoretical correlation between the mass fraction and the Capillary number, and the agreement between his predictions and Cox's experiments is good in the range of $10^{-3} < Ca < 10^{-2}$.

Some contributions found in the literature deal with the theoretical modeling of gas-liquid displacement in the small gap between two parallel plates. Giavedoni and Saita (1987) reviewed these articles and presented a theoretical analysis

of the steady displacement of a viscous liquid by a semi-infinite gas bubble using finite element method. They extended the range of the Capillary number of the analysis from 5×10^{-5} up to 10. Lee et al. (2002) used a finite-element method to study the steady gas displacement of a polymeric liquid confined between two parallel plates. The non-Newtonian behavior of the liquid was modeled by three different differential constitutive equations. Articles dealing with the analysis of liquid-liquid displacement are much scarcer. One of these few papers is given by Goldsmith and Mason (1963), who report experimental results on the amount of displaced liquid left on the tube wall as a function of different parameters. In their experiments, the displacing material is a long drop of a viscous liquid. The results showed that the mass fraction rises as the viscosity ratio $N_\mu = \mu_2/\mu_1$ is decreased, where the index 1 refers to the displacing fluid and μ_2, to the displaced fluid. This trend agrees with the theoretical predictions and experimental data presented in this work. Teletzke et al. (2002), using a perturbation method, analyzed the wetting hydrodynamics problem. They extended the work of Bretherton (1961) to account for a viscous (rather than inviscid) displacing fluid, and the effects of intermolecular forces in submicroscopically thin films. Their computations agreed with the observation of Goldsmith and Mason (1963), which showed that the film thickness of the displaced fluid left on the wall rises with the viscosity of the displacing fluid. However, their results were limited to small capillary numbers, namely, $Ca < 10^{-4}$.

Petitjeans and Maxworthy (1996) analyzed the situation of liquid-liquid displacement with miscible liquids. They studied the effect of the Peclet number, defined as $Pe = V_m D/D_m$, where V_m is the maximum velocity far from the tip of the interface, D the tube diameter, and D_m is the diffusion coefficient. The high Peclet number regime should correspond to the case of immiscible fluids and infinite capillary number.

Soares et al. (2005), studied the case where a Newtonian viscous liquid was displaced by a long drop of another Newtonian viscous liquid in a capillary tube. The problem was analyzed by numerical simulations and experiments for some governing parameters. The authors investigated the capillary number and viscosity ratio effects on the fractional deposited mass, *m*. They also analyzed the stream line patterns and the shape of the interface tip.

The present work consists of a continuation of previous work of Soares et al. (2005) and Mesquita et al (2006). The major difference of these works is the fact that numerical simulations were performed to investigate non-Newtonian effects when a polymeric material is used as the displacing fluid.

A thin layer of the displaced liquid is left behind on the tube walls, as illustrated in Fig.(1). In the figure, R_0 is the radius of the tube and R_b the radius of the cylindrical portion of the interface. The theoretical approach consisted of the solution of the governing equations of this free surface problem using the finite element method. The flow field variables and the position of the interface between the two liquids are all solved simultaneously and the formulation is not limited to low capillary numbers. The theoretical predictions show the effect of different parameters on the interface configuration and on the thickness of the layer of the displaced liquid left on the walls. It is important to notice that, a main hypothesis considered is that we study the problem far from the limit of instability effects. Depending on the wetability, the dimensionless lenght of the drop and the other dimensionless parameters of the problem indicated below, the problem becomes unstable. The stability analysis associated with the physical problem is still in order.

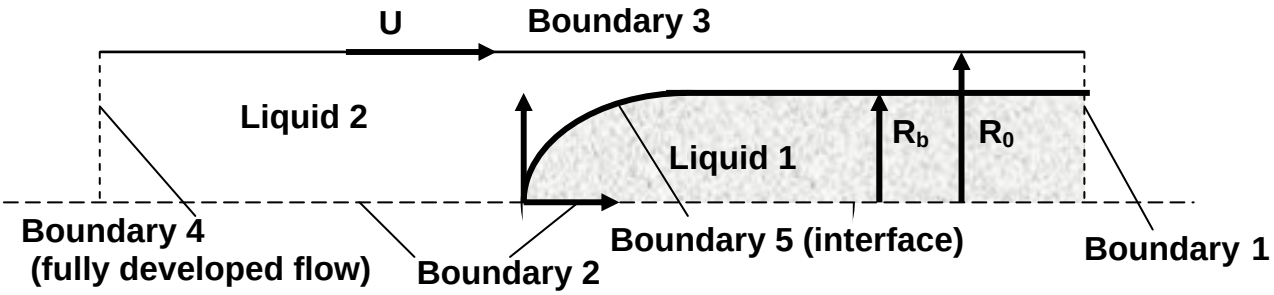

Figure 1 – Schematics of the problem.

2. MATHEMATICAL FORMULATION

2.1. Conservation equations and boundary conditions

The physical model to describe the displacement of a Newtonian liquid of viscosity μ_2 by a long drop of a second non-Newtonian liquid of viscosity η_1 is now presented. The displacing drop (liquid 1) is translating steadily with speed U. To simply the analysis, the governing equations are written with respect to a moving reference frame located at the tip of the interface. In this frame of reference, the flow is steady and the wall is moving with velocity U.

The geometry analyzed is an axisymmetric tube of radius R_0. The liquid is assumed to be incompressible, and the flow is laminar and the inertia is negligible.The velocity and pressure fields are governing by the continuity and momentum equations. In cylindrical coordinates, these governing equations are written as (the subscript $k = 1,2$ labels the two liquids).

$$0 = \frac{1}{r}\frac{\partial}{\partial r}\left(r v_k\right) + \frac{\partial}{\partial x}\left(u_k\right) \tag{2}$$

$$0 = \left[\frac{1}{r}\frac{\partial}{\partial r}\left(r\tau_{(rx)_k}\right) + \frac{\partial}{\partial x}\left(\tau_{(xx)_k}\right)\right] - \frac{\partial p_k}{\partial x} \tag{3}$$

$$0 = \left[\frac{1}{r}\frac{\partial}{\partial r}\left(r\tau_{(rr)_k}\right) - \frac{\tau_{(\theta\theta)_k}}{r} + \frac{\partial}{\partial x}\left(\tau_{(rx)_k}\right)\right] - \frac{\partial p_k}{\partial r} \tag{4}$$

Where u and v are respectively the axial and radial components of the velocity field $\boldsymbol{u}$ and the quantities $\tau_{xx}, \tau_{yy}, \tau_{rx}, \tau_{ry}$ and $\tau_{\theta\theta}$ are the components of the stress tensor $\boldsymbol{\tau}$.
In order to facilitate the following description of the boundary conditions, the boundaries are labeled from 1 to 5, as illustrated in Fig. (1).

1) Far enough upstream of the interface, Boundary 4, the flow is taken to be fully developed and the pressure is assumed to be uniform:

$$\mathbf{n}\cdot\nabla\mathbf{u}_2 = 0, \;\; p_2 = p_{in} \tag{5}$$

where $\boldsymbol{n}$ is the unit vector normal to the boundary surface and p_{in} the pressure field.

2) Far enough downstream, Boundary 1, the flow is also assumed to be fully developed, but the pressure is not imposed:

$$\mathbf{n}\cdot\nabla\mathbf{u}_1 = 0 \tag{6}$$

3) Along the symmetry axis, Boundary 2, both the shear stress and the radial velocity vanish:

$$\mathbf{t}\cdot\left[\mathbf{n}\cdot\boldsymbol{\tau}_k\right] = \tau_{(rx)_k} = 0\,, \;\; \mathbf{n}\cdot\mathbf{u}_k = 0 \tag{7}$$

where $\boldsymbol{t}$ is a unit vector tangent to the boundary surface.

4) The no-slip and impermeability conditions are imposed along the tube wall, Boundary 3:

$$\mathbf{u} = U\mathbf{e}_x \tag{8}$$

where $\boldsymbol{e}_x$ is the unit vector in the x-direction.

5) At the liquid-liquid interface, Boundary 5, the traction balances the capillary pressure, and there is no mass flow across the interface:

$$\mathbf{n}\left(p_1 - p_2\right) + \mathbf{n}\left(\boldsymbol{\tau}_2 - \boldsymbol{\tau}_1\right) = \frac{\sigma}{R_m}\mathbf{n} \tag{9}$$

$$\left(\mathbf{u}_1 - \mathbf{u}_2\right) = 0 \tag{10}$$

In Eq. (9), $1/R_m$ is the local mean curvature of the interface, defined as

$$\frac{1}{R_m}\mathbf{n} = \frac{1}{\sqrt{x_s^2 + r_s^2}}\frac{\partial \mathbf{t}}{\partial s} - \frac{x_s}{r\sqrt{x_s^2 + r_s^2}}\mathbf{n} \tag{11}$$

where $\boldsymbol{t}$ is the unit tangent vector to the free surface, s is the arc-length curvilinear coordinate along the interface in the r-x plane and $x_s = \partial x / \partial s$ and $r_s = \partial r / \partial s$ are spatial derivatives with respect to s.

2.2. Constitutive equations

In order to close the set of differential equations, the stress tensor was related with the kinematics of the flow by the Generalized Newtonian Fluid model. In this model, the stress tensor is given by

$$\mathbf{T} = -p\mathbf{I} + \eta(\dot{\gamma})\dot{\boldsymbol{\gamma}} \tag{12}$$

where $\dot{\boldsymbol{\gamma}} = \nabla\mathbf{u} + \nabla\mathbf{u}^{\mathrm{T}}$ is the rate of strain tensor. The scalar quantity $\eta(\dot{\gamma})$ is the viscosity function, and $\dot{\gamma} \equiv \sqrt{\frac{1}{2} tr(\dot{\boldsymbol{\gamma}} \cdot \dot{\boldsymbol{\gamma}})}$ is the deformation rate. The viscosity function $\eta(\dot{\gamma})$ is that proposed by Papanastasiou (1987) anddescribed by Eq. (13).

$$\eta = \mu + \frac{\tau_0(1 - e^{-c\dot{\gamma}})}{\dot{\gamma}} \tag{13}$$

where τ_0 is the yield stress, μ is an asymptotic viscosity value at high shear rate and c is a regularization parameter. A viscoplastic material is generally described as a material which flows only when the stress is above a particular level, amaterial with a yield stress. The Bingham model which was the first model proposed to capture such behavior has the inconvenient feature of being discontinuous and, therefore, it leads to numerical difficulties. Papanastasiou (1987) proposed the use of a regularization parameter in order to have a smooth transition between non-yielded and yielded state. As suggested by a number of works presented on literature, for a value of the regularization parameter *c=1000*, Papanastasiou´s model closely describes the behavior of Bingham material and, therefore, this value is adopted in the present work.

3.SOLUTION METHOD

3.1 The free boundary problem

Due to the free surface, the flow domain is unknown a priori. In order to solve this free-boundary problem by means of standard techniques for boundary value problems, the set of differential equations and boundary conditions written for the physical domain has to be transformed to an equivalent set, defined in a known reference domain. This subject is better discussed on papers of Kistler and Scriven (1983) and de Santos (1991). This transformation is made by a mapping $\mathbf{x} = \mathbf{x}(\boldsymbol{\xi})$ that connects the two domains, as shown in Fig. (2). A functional of weighted smoothness can be used successfully to construct the type of mapping involved here. The inverse of the mapping that minimizes the functional is governed by a pair of elliptic differential equations that are identical to those encountered in diffusional transport with variable diffusion coefficients. The coordinates ξ and η of the reference domain satisfy

$$\nabla \cdot (D_\xi \nabla \xi) = 0 \text{ and } \nabla \cdot (D_\eta \nabla \eta) = 0 \tag{14}$$

where D_η and D_ξ are diffusion-like coefficients used to control gradients in coordinate potentials, and thereby the spacing between curves of constant ξ on the one hand and of constant η on the other that make up the sides of the elements that were employed; they were quadrilateral elements. Eq. (14) describe the inverse mapping $\xi(x)$. To evaluate $x = x(\xi)$, the diffusion equations that describe the mapping also have to be transformed to the reference configuration.

The gradient of the mapping $x = x(\xi)$ in a two dimensional domain is defined as $\nabla_\xi x = \mathbf{J}$, and $\|J\| = \det \mathbf{J}$ is the Jacobian of the transformation. Boundary conditions are needed in order to solve the second-order partial differential equations (14). Spatial derivatives with respect to the coordinates of the physical domain ***x*** can be written in terms of the derivatives with respect to the coordinates of the reference domain ξ by using the inverse of the gradient of the mapping

$$\begin{pmatrix} \partial/\partial x \\ \partial/\partial y \end{pmatrix} = J^{-1} \begin{pmatrix} \partial/\partial \xi \\ \partial/\partial \eta \end{pmatrix} \tag{15}$$

Along the solid walls and synthetic inlet and outlet planes, the boundary is located by imposing a relation between coordinates *x* and *y*, and stretching functions are used to distribute the nodal points of the finite element mesh along the

boundaries. The free boundary (gas-liquid interface) is located by imposing the kinematic condition, Eq. (6). The discrete version of the mapping, Eq. (14), is generally referred to as mesh generation equations.

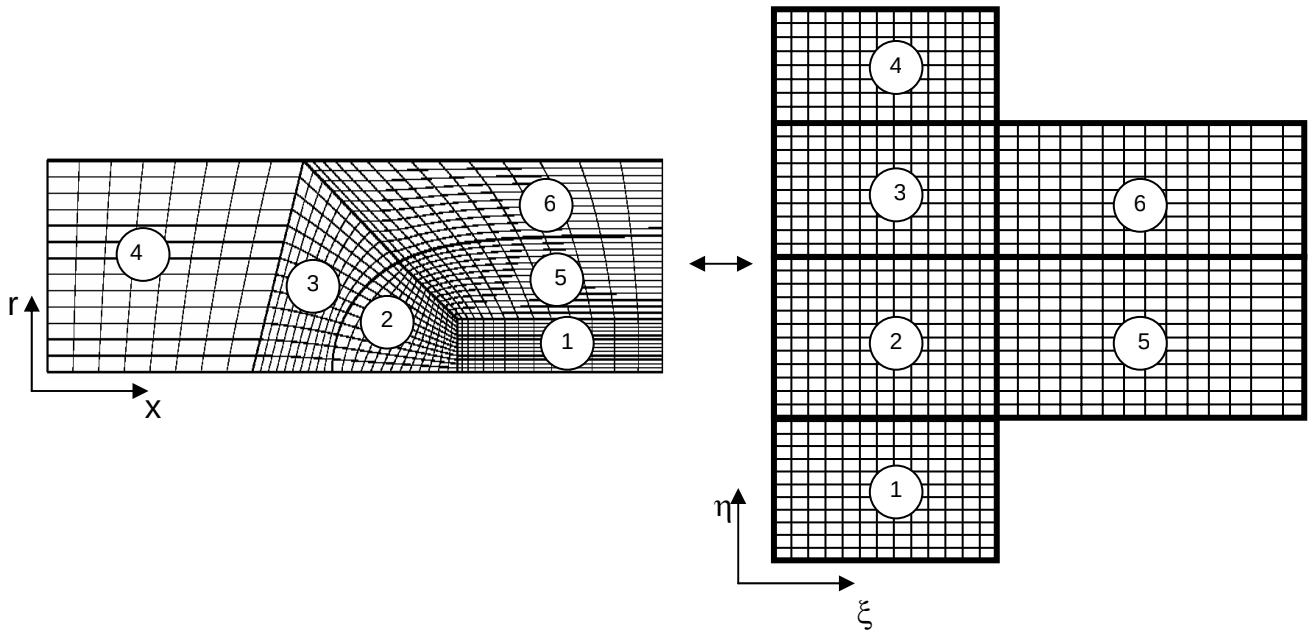

Figure 2 – Mapping between the physical and reference domains.

3.2 Solution of the equation system by Galerkin / Finite Element Methods

The differential equations that govern the problem and the mapping (mesh generation) equations were solved all together by the Galerkin/Finite Element Method. Biquadratic basis functions (ϕ_j) were used to represent the velocity and nodal coordinates, while linear discontinuous functions (χ_j) were employed to expand the pressure field. The velocity, pressure and node position are represented in terms of appropriate basis functions.

$$u = \sum U_j \phi_j ; v = \sum V_j \phi_j ; p = \sum P_j \chi_j ; x = \sum X_j \phi_j ; r = \sum R_j \phi_j \tag{16}$$

The coefficients of the expansions are the unknown of the problem:

$$C = \left[U_j \;\; V_j \;\; \mathrm{P_j} \;\; \mathrm{X_j} \;\; \mathrm{R_j} \right]^T \tag{17}$$

The corresponding weighted residuals of the Galerkin method related to conservation of momentum, mass and mesh generation are:

$$R^i_{mx} = \int_{\bar{\Omega}} \left[\frac{\partial \phi_i}{\partial x} T_{(xx)_k} + \frac{\partial \phi_i}{\partial r} T_{(xr)_k} \right] r \|J\| d\bar{\Omega} - \int_{\bar{\Gamma}} \mathbf{e}_x \left(\mathbf{n} \cdot \mathbf{T}_k \right) \phi_i r \frac{d\mathbf{\Gamma}}{d\bar{\mathbf{\Gamma}}} d\bar{\mathbf{\Gamma}} \tag{18}$$

$$R^i_{mr} = \int_{\bar{\Omega}} \left[\frac{\partial \phi_i}{\partial x} T_{(xr)_k} + \frac{\partial \phi_i}{\partial r} T_{(rr)_k} + \frac{\phi}{r} T_{\theta\theta_k} \right] r \|J\| d\bar{\Omega} - \int_{\bar{\Gamma}} \mathbf{e}_r \left(\mathbf{n} \cdot \mathbf{T}_k \right) \phi_i r \frac{d\mathbf{\Gamma}}{d\bar{\mathbf{\Gamma}}} d\bar{\mathbf{\Gamma}} \tag{19}$$

$$R^i_c = \int_{\bar{\Omega}} \left[\frac{1}{r} \frac{\partial}{\partial r} (r v_k) + \frac{\partial u_k}{\partial x} \right] \chi_i r \|J\| d\bar{\Omega} \tag{20}$$

$$R^i_\xi = -\int_{\bar{\Omega}} D_\xi \left(\frac{\partial \phi}{\partial x} \frac{\partial \xi}{\partial x} + \frac{\partial \phi}{\partial r} \frac{\partial \xi}{\partial r} \right) \|J\| d\bar{\Omega} + \int_{\Gamma} D_\xi \left(\nabla \xi \cdot \mathbf{n} \right) \phi_i \frac{d\mathbf{\Gamma}}{d\bar{\mathbf{\Gamma}}} d\bar{\mathbf{\Gamma}} \tag{21}$$

$$R^i_\eta = -\int_{\bar{\Omega}} D_\eta \left(\frac{\partial \phi}{\partial x} \frac{\partial \eta}{\partial x} + \frac{\partial \phi}{\partial r} \frac{\partial \eta}{\partial r} \right) \|j\| d\bar{\Omega} + \int_{\Gamma} D_\eta \left(\nabla \eta \cdot \mathbf{n} \right) \phi_i \frac{d\mathbf{\Gamma}}{d\bar{\mathbf{\Gamma}}} d\bar{\mathbf{\Gamma}} \tag{22}$$

3.3 Solution of the non-linear system of algebraic equation by Newton's Method

As indicated above, the system of partial differential equations and boundary conditions is reduced to a set of simultaneous algebraic equations for the coefficients of the basis functions of all the fields. This set is non-linear and sparse. It was solved by Newton's method. In order to improve the initial guess there were necessary to solve intermediate problems. The first successful free surface flow was computed using a fixed boundary flow field with slippery surface in place of the free boundary as the initial condition for Newton's method. The linear system of equations at each Newton iteration was solved using a frontal solver. A mesh convergence analysis was done increasing the elements number until the solution changed by less that 1% between successive refinements. The domain was divided into 880 elements that correspond to 3635 nodes and 17180 degrees of freedom. A representative mesh is shown in Fig (3).

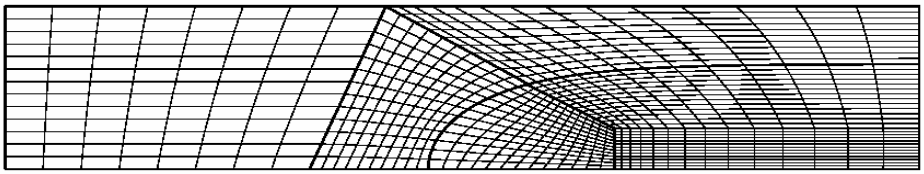

Figure 3 – The finite element mesh, with 880 elements and 17180degrees of freedom.

4. RESULTS

The amount of the liquid 2 that remains on the capillary wall is usually reported in terms of the mass fraction of liquid that is not displaced m, or simply by the liquid film thickness left on the wall. The two forms are related by

$$m = \frac{\text{mass left on wall}}{\text{total mass}} = 1 - \frac{\text{displaced mass}}{\text{total mass}} \partial$$
$$= 1 - \left(\frac{D_b}{D_0}\right)^2 = 1 - \left(1 - \frac{2h_\infty}{D_0}\right)^2 \tag{23}$$

The mass fraction of the liquid 2 left on the tube wall can be evaluated using the mass conservation principle for the liquid 2 in a control volume containing the tip of the interface and attached to it. Figure (4) shows this control volume and the sketch of the velocity profiles at inlet and outlet plane as seen from a reference frame attached to tip of the interface. The mass flow rate of the liquid 2 through the control surface upstream of the drop is equal to $\pi R_0^2 \bar{u}^*$ and through the control surface downstream the tip of the interface is $\pi\left(R_0^2 - R_b^2\right)\bar{U}$, $\bar{u}^*$ and $\bar{U}$ being the average velocities of the liquid 2 at the two planes with respect to the moving frame of reference.

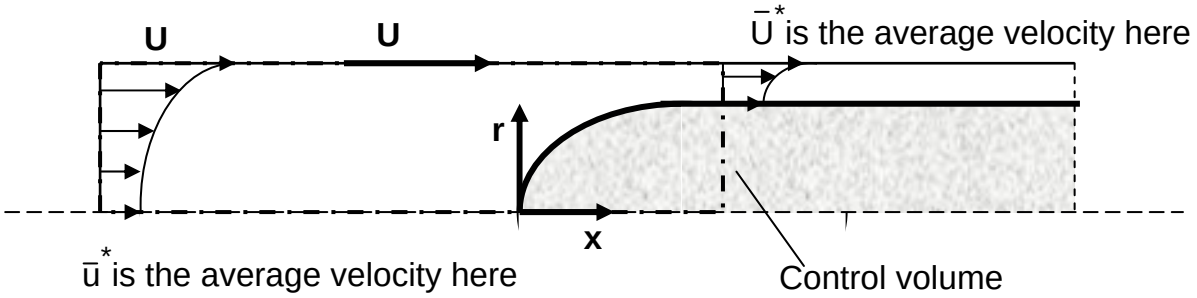

Figure 4 –Velocity profile as measured from a reference frame at the tip of the interface.

The average velocity with respect to the moving frame of reference $\bar{u}^*$ can be evaluated as a function of the average velocity with respect to a fixed frame of reference, $\bar{u}^* = U - \bar{u}$. Combining the previous relations, the mass fraction m can be expressed in terms of the average velocities.

$$m = 1 - \left(\frac{D_b}{D_0}\right)^2 = \frac{U - \bar{u}}{\bar{U}} \tag{24}$$

For a Newtonian liquid displacement of a no inertial incompressible Newtonian liquid, the relevant dimensionless parameters that govern the problem are the Capillary number (Ca) and Viscosity ratio (N_μ). The Capillary number and viscosity ratio are given by

$$Ca \equiv \frac{\mu_2 U}{\sigma} \tag{25}$$

$$N_\mu \equiv \frac{\mu_2}{\mu_1} \tag{26}$$

On the other hand, when the displaced liquid is non –Newtonian, the *Ca* is, again, calculated by Equation (25), but, N_μ must be redefined. It is necessary to choose a characteristic viscosity of the problem. For this purpose the viscosity function is evaluated at the characteristic deformation rate of the flow which is in this problem $\dot{\gamma}_c = V_b / R$. Hence, the viscosity ratio for the power-law fluid is given by

$$N_\eta = \frac{\mu_2}{\eta_c} = \frac{\mu_2}{\mu + \dfrac{\tau_0\left(1 - e^{-1000\dot{\gamma}}\right)}{\dot{\gamma}}} \tag{27}$$

The rheological dimensionless parameter is the dimensionless yield stress (τ_0') is given by

$$\tau_0' = \frac{\tau_0}{\tau_c} = \frac{\tau_0}{\mu\dot{\gamma}_c + \tau_0} = \frac{\tau_0}{\mu\left(V_b / R\right) + \tau_0} \tag{28}$$

In order to validate the present work, the results are compared with the experiments from Taylor (1961) and Cox (1962) and numerical solution obtained by Souza et al (2006) for gas-liquid displacement, these results are shown in Figure (5). The agreement is quite good over the range of capillarity numbers explored.

Figure (6) presents the values of the fraction of mass deposited on the tube wall as a function of the capillary number at fixed viscosity ratio, $N_\mu = 4$, for liquid-liquid displacement of two Newtonian fluids. Figure (6) shows a good agreement with the results of Soares et al (2006).

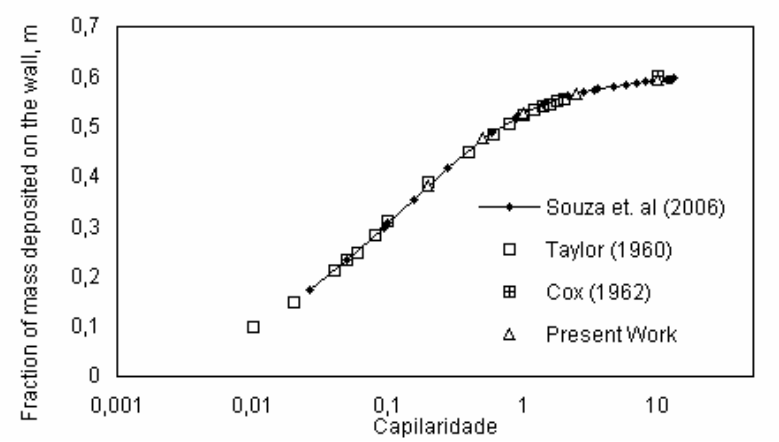

Figure 5 – Fraction of mass deposited on the tube wall as a function of the capillary. Experimental and Numerical predictions for gas displacing a Newtonian liquid.

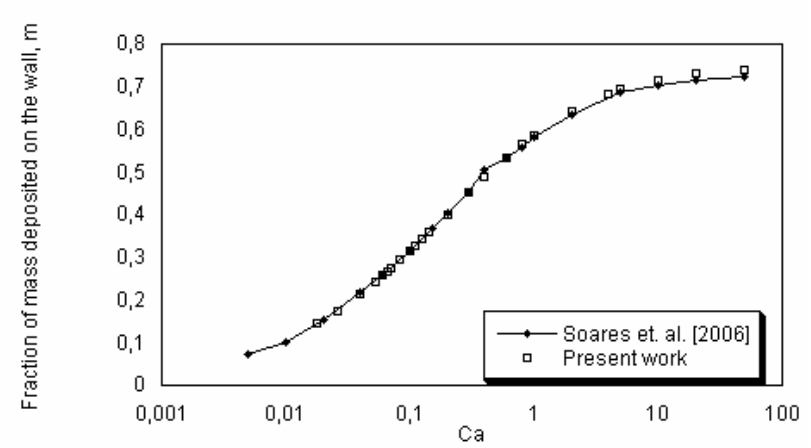

Figure 6 - Fraction of mass deposited on the tube wall as a function of the capillary for two Newtonian liquids. Numerical predictions at fixed viscosity ratio $N_\mu = 4$.

Figure (7) presents the fraction of mass deposited on the tube wall as a function of the dimensionless yield stress (τ_0'). The results indicate that as τ_0' becomes higher the fraction of mass deposited on the tube wall decreases.

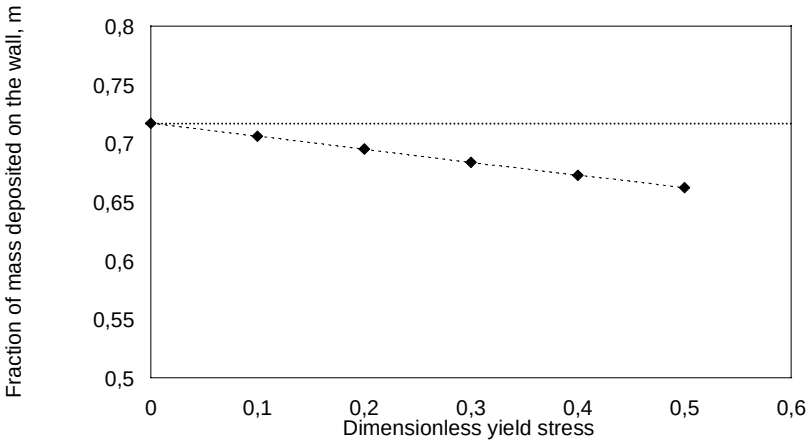

Figure 7 - Fraction of mass deposited on the tube wall as a function of the dimensionless yield-stress. Numerical predictions at fixed capillary number, Ca=10, and viscosity ratio, $N_\mu = 4$.

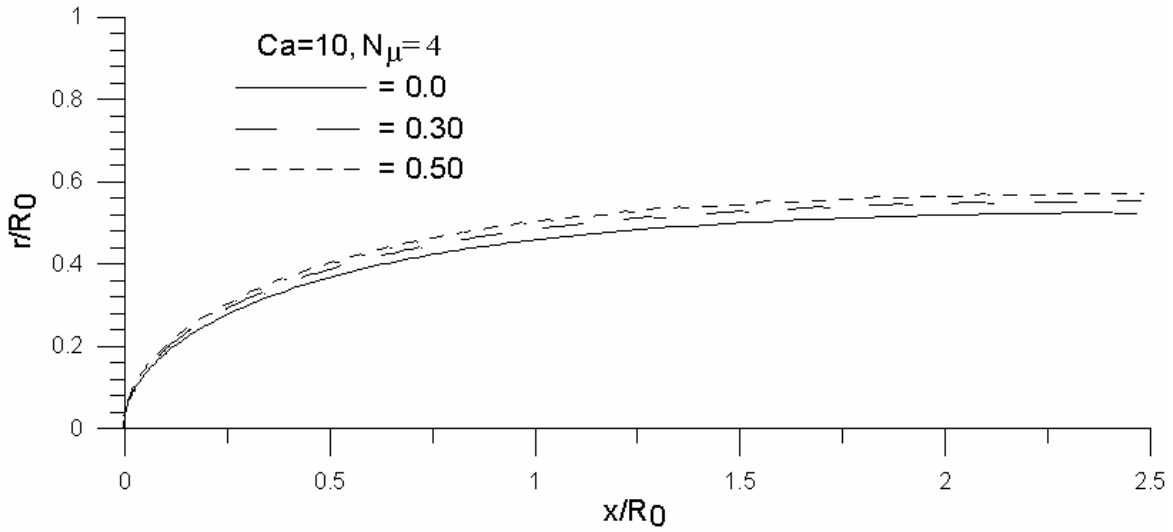

Figure 8 - Free surface profile at Ca=10 and $\tau_0' = 0.0, 0.30$ *and* 0.50.

5. Conclutions

An axisymmetric model of the flow near the upstream liquid-liquid interface of a long drop penetrating through a liquid in a capillary tube was presented. The presence of the interface makes the problem complex, since the domain in which the differential equations are integrated is unknown a priori. A fully coupled formulation was used and the differential equations were solved via the Galerkin finite element method.

Recent articles are found in the literature which analyze liquid displacement in tubes. However, these are limited to gas-liquid displacement or to liquid-liquid displacement at rather small capillary Numbers and for two Newtonian fluids. Thus, the main contribution of the present work was to investigate the influence of the dimensionless yield stress of the displacing liquid on the fraction of mass deposited on the tube wall for a fixed capillary number and viscosity ratio.

The predictions showed a decrease of fractional mass left behind with increase of the τ_0'. Hence, the viscoplastic material seems to be a more efficient displacing liquid in oil recovery then the Newtonian one.

6. References

Bretherton, F. P., 1961, "The Motion of Long Bubbles in Tubes," Journal of Fluid Mechanics, Vol. 10, pp. 166–188.

Cox, B. G., 1962, "On Driving a Viscous Fluid Out of a Tube," Journal of Fluid Mechanics, Vol. 14, pp. 81–96.

Dimakopoulos, Y. and Tsamopoulos, J., 2003, "Transient Displacement of a Viscoplastic Material by Air in Straight and Constricted tubes", Journal of Non-Newtonian Fluid Mechanics, Vol. 112, pp. 43-75.

Fairbrother, F., and Stubbs, A. E.,1935, "Studies in Electroendosmosis. Part VI. The Bubble-Tube Methods of Measurement," J. Chem. Soc., Vol. 1, pp. 527–529.

Giavedoni, M. D., and Saita, F. A., 1997, "The axisymmetric and plane cases of a gas phase steadily displacing a Newtonian liquid: A simultaneous solution of the governing equations," Phys. Fluids, 9, pp. 2420-2428.

Goldsmith, H. L. and Manson, S.G., 1963, "The Flow of suspensionsthrough tubes," J. Colloid Sci., 18, pp. 237-261.

Lee, A. G., Shaqfeh, E.S. G., and Khomami, B., 2002, " A study of viscoelastic free surface flows by finite element method: Hele-Shaw an Slot Coating Flows," J. Non-Newtonian Fluid Mech., 108, pp.327-362.

Petitjeans, P., and Maxworthy, T., 1996, ''Miscible Displacements in Capillary Tubes,'' J. Fluid Mech., 326, pp. 37–56.

Mesquita, M. S., Soares, E.J., Thompson, R. L., Carvalho, M. S., Souza Mendes, P. R., 2006, "Liquid Recovery In Capillary Tubes by Injection of A Power-Law Material, submitted to IV Congresso Nacional de Engenharia Mecânica, CONEM 2006.

Papanastasiou, T., C., 1987, "Flows of Materials with Yield-Stress", Journal of Rheology, Vol.31 pp. 385-404.

Soares, E. J., Carvalho, M. S., Souza Mendes, P. R., 2005, "Immiscible liquid-liquid displacement in capillary tubes," Journal of Fluids Engineering, Vol. 127 (1), pp. 24-31.

Taylor, G. I., 1961, "Deposition of a Viscous Fluid on the Wall of a Tube", Journal of Fluid Mechanics, Vol. 10, pp. 161–165.

Souza, D. A., Soares, E. J., Queiroz, R. S. and Thompson, R. L., 2006, " Numerical investigation on gas-displacement of a shear-thinning liquid and a viscoplastic material in capillary tubes", submitted to International Journal of Multiphase Flow.

Teletzke, G. F., Davis, H. T., and Scriven, L. E., 1988, ''Wetting Hydrodynamics,'' Rev. Phys. Appl., 23, pp. 989–1007.

7. Copyright Notice